ACS APPLIED ENERGY MATERIALS

www.acsaem.org Article

Optimal Dye Sensitized Solar Cell and Photocapacitor Performance with Efficient Electrocatalytic SWCNH Assisted Carbon Electrode

Gurulakshmi Maddala, Meenakshamma Ambapuram, VijayaLaxmi Tankasala, and Raghavender Mitty*

Cite This: *ACS Appl. Energy Mater.* 2021, 4, 11225−11233 Read Online

ACCESS | Metrics & More | Article Recommendations | Supporting Information

ABSTRACT: The present work demonstrates the high photovoltaic power conversion efficiency (PCE) of 11.12% using single wall carbon nanohorn assisted carbon counter electrode based dye sensitized solar cells (DSSCs), which demonstrates a superior PCE compared to that of platinum (9.41%). This superior performance was a motivation to fabricate a dye sensitized solar module (DSSM) consisting of six series connected DSSCs arranged in a bifacial manner toward the application of building integrated photovoltaics. The DSSM demonstrated a remarkable, champion PCE of 19.71%. This high PCE, driven to fabricate an integrated device (photocapacitor), consists of a DSSM and a supercapacitor (SC). Upon two-sided illumination, the DSSM generated electrical power, and the same power is used for charging the supercapacitor. A working light emitting diode is demonstrated with discharge of the SC. The detailed fabrication strategies and results are discussed.

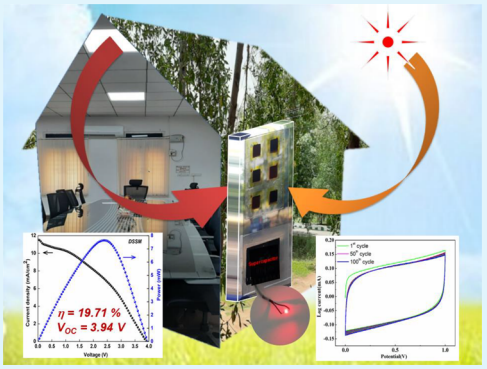

KEYWORDS: *cost-effective carbon electrode, screen print, platinum-free, single wall carbon nanohorns, spray coat, dye sensitized solar cell, bifacial, DSSM, supercapacitor, photocapacitor*

1. INTRODUCTION

The global energy requirement is crucial, and it can potentially be addressed through a clean energy conversion photovoltaic technology. Cost-effective, third-generation solar photovoltaics have become significant, so attention has been paid due to its easier fabrication process, environmental friendliness, and good energy conversion efficiency. The dye sensitized solar cell (DSSC) is identified as an affordable photovoltaic technology and has attracted more attention for its capability to deliver low-cost power generation.[1−3] DSSC consists of a photoelectrode (PE) of dye anchored TiO_2 nanoparticles, an electrolyte comprising redox couples (generally, I^-/I_3^-), and a counter electrode (CE). Counter electrodes play a critical role in achieving high power conversion efficiency (PCE). Developing a potential CE is essential, as CE catalysts have high conductivity, have good catalytic activity, are more stable, etc. Generally, a very thin platinum (Pt) layer will be deposited onto a conductive fluorine doped tin oxide (FTO) coated glass substrate which is used as the counter electrode, due to its extreme catalytic performance for tri-iodide reduction and good electrical conductivity.[4,5] Due to its higher cost, rare availability leads to minimal large-scale production for power production. To overcome this, efforts have been made by researchers for the development of cost-effective catalysts, include carbonaceous materials, nitride, sulfides, etc., as promising catalysts materials.[6−13] The present research focuses on a Pt-free, cost-effective CE as an alternative to the "champion" CE. The present study aims to develop an effective, potential CE through an easy preparation processes.

Numerous carbon-oriented materials like active carbon,[14] carbon powder,[15,16] carbon spheres,[17,18] and fullerenes[19] have been used as CEs which have shown remarkable progress. The performance of DSSCs fabricated with carbon-oriented CEs are lower compared to Pt based CEs. Improved electrocatalytic active sites through deposition of another material over CE catalysts could result in higher performance.[20] The single wall carbon nanohorn (SWCNH) based CE assisted DSSC exhibited a good PCE.[21−25]

The development of bifacial DSSM provides a potential candidate for building integrated photovoltaics (BIPVs).[26−29] The bifacial BIPV structure enables light energy from direct sunlight (coming from outside) and diffused light (indoor light) to be converted into electric power. DSSCs are recognized as the best choice for indoor light conversion (~ 200−1000 lx radiance).[30−34] The DSSC is an ideal substituent for charging in tiny electronic gadgets under indoor light conditions. The DSSC combined with a battery or supercapacitor acts as a self-powered system, demonstrating its

Received: July 15, 2021
Accepted: September 20, 2021
Published: September 30, 2021

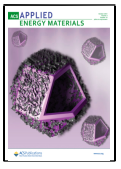

https://doi.org/10.1021/acsaem.1c02087
ACS Appl. Energy Mater. 2021, 4, 11225−11233

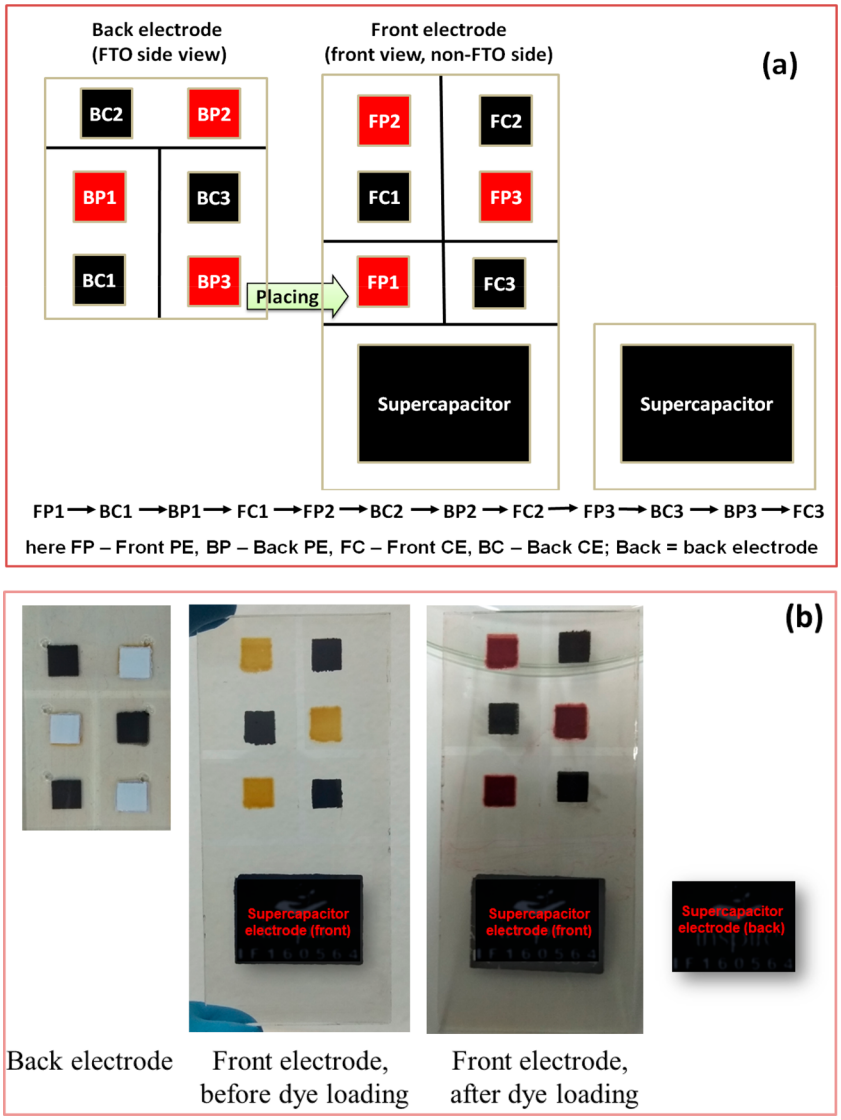

Figure 1. (a) Back and front DSSM glass after proper removal of the FTO layer (black line); and (b) resultant electrodes after material coatings.

advancement.[35] Many approaches are being attempted to improve the performance of self-powered systems.[36,37]

Photocapacitors are emerging as promising, self-sufficient energy devices consisting of solar cells and supercapacitors. Over the past few years, researchers are focusing on the development of high-performance photocapacitors with higher energy density and good specific capacitance. The photocapacitor is capable of converting the electromagnetic radiation from the sun into electricity and storing the converted power. Most commonly, reported studies reveal a single solar cell charging a supercapacitor (SC). This limits the final voltage of the storage section such that it is not sufficient to drive most applications, like low-power electronics. To address this concern, here we proposed a device that consists of a bifacial DSSM (constituted series of six DSSCs) as a light harvester and an ionic liquid based supercapacitor as a storage unit. The two efficient SWCNH/carbon assisted identical electrodes are used for SC fabrication and are filled with an ionic $EMIBF_4$ electrolyte. Upon two-sided illumination of the bifacial DSSM, the delivered voltage is used for charging the supercapacitor.

Here, SWCNH supported carbon is used as the CE for the DSSC as well as for SC electrodes. The DSSM delivered a V_{oc} of 3.94 V with an overall efficiency of 19.71%. The enhanced performance is reflected from its higher conductivity, excellent electrochemical properties, and the high current density of SWCNH/carbon CEs.

2. EXPERIMENTAL SECTION

Photoelectrode Preparation. Photoelectrodes were prepared by the procedure discussed here. First, FTO (fluorine doped tin oxide) (Greatcell Solar, TEC7, 7 Ω/square) conducting glass substrates were carefully washed with detergent liquid and eroded in sequence with deionized water, absolute ethanol, acetone, and finally 2-propanol for 10 min each to eliminate organic contaminants if any. A compact film of titanium dioxide solution (Solaronix, T-L/SC) was layered over a cleaned FTO glass substrate, which was then heated to 70 °C for 30 min. A 13−15 μm TiO_2 film is realized by screen printing 18 NR-T transparent titanium dioxide paste (18-NR, Greatcell Solar) and sintering to 500 °C (30 min). The treatment of a compact layer like that described above is again repeated. Then, the substrates were cooled to 100 °C and immersed in a solution of N719 dye (0.3 mM in absolute ethanol) in dark conditions for 16 h. Finally, electrodes were washed gently with ethanol to remove any unanchored molecules of N719 dye.

Counter Electrode Preparation, Test Cell (DSSC) Assembly. The carbon based counter electrodes were prepared via screen print

https://doi.org/10.1021/acsaem.1c02087
ACS Appl. Energy Mater. 2021, 4, 11225−11233

by use of a commercial carbon paste (Solaronix) and sintered to 500 °C. A solution containing 5 mg of SWCNH dispersed in 2-propanol was spray coated over a carbon coated FTO glass substrate at 100 °C to get SWCNH/carbon counter electrodes. For comparison, platinum based CEs were prepared (spin coating of a Pt solution at 2000 rpm, sintered to 500 °C).

The closed type individual test cell (DSSC) was fabricated by a sandwich of photoelectrodes and counter electrodes, with thermal adhesive film (Solaronix, 25 μm, polymer melt film) placed in between, pressed gently on a hot plate while heating at 110 °C. Altered HI-30 electrolyte was injected via the technique of back vacuum, and holes at CEs were closed through the polymer melt film and cover glass.

Dye Sensitized Solar Module (DSSM) Fabrication and Integration with Supercapacitor. *Front Electrode Preparation.* Glass substrates (FTO conducting) of 8.5 × 4 cm^2 size were taken and etched properly using zinc dust and HCl to disconnect electrically from one to another part as shown in Figure 1a (black lines indicate the FTO removed part). Initially, glass substrates were cleaned in ethanol and acetone in an ultrasonicator for 10 min. A 5 μm thick carbon film was deposited to act as CE (FC1, FC2, FC3, and supercapacitor part, one electrode) using a screen print technique and heated to 100 °C. Over FC1, FC2, and FC3, SWCNHs solution (in 2-propanol) was spray coated and heated to 100 °C. As the other parts on the front electrode are treated, TiO_2 paste was then deposited (FP1, FP2, FP3) by using a screen print technique, along with sintering to 500 °C for 30 min to remove binders and solvents to electrically interconnect well with the respective nanoparticles. Then, the electrode was soaked for 16 h in 0.3 mM N719 dye in ethanol solution. While soaking, the carbon part (FC1, FC2, FC3 and supercapacitor part) is sealed with Kapton tape and Surlyn to avoid damage of carbon.

Back Electrode Preparation. FTO glass substrates of 5 × 3.5 cm^2 size were used, to have additional space for the electrode contact for measurements and etched properly to disconnect electrically from one to another part as shown in Figure 1a (black lines specify the FTO removed part). Six inlet holes of approximately 0.5 mm diameter were drilled (shown in Figure 1b) for electrolyte filling. FTO glass substrates were cleaned, and carbon films were deposited for CE parts (BC1, BC2, BC3) using screen printing and heated to 100 °C. Over BC1, BC2, and BC3, SWCNH solution was sprayed and heated to 100 °C. As the other parts on the back electrode, TiO_2 paste was then deposited (BP1, BP2, BP3) by using a screen printer and then sintered to 500 °C for 30 min. Before dye soaking, the carbon part (BC1, BC2, BC3) was sealed with Kapton tape and Surlyn to avoid damage of the carbon. Then, the electrode was soaked for 16 h in 0.3 mM N719 dye in ethanol solution, and the resulting electrode is shown in Figure 1b as after dye loading.

Assembling of DSSM. These front and back electrodes were sealed by placing a thermal adhesive film (Solaronix, polymer melt film) with a gentle hot press up to 110 °C. An acetonitrile (AcN) based redox coupled altered electrolyte (altered HI-30) was injected using a back vacuum filling technique via 6 holes followed by its perfect seal.

Integrated Device. Another FTO glass substrate of size 3.5 × 4 cm^2 was cleaned thoroughly, and the carbon paste was screen printed (deposition area 2 × 3 cm^2) and heated to 100 °C. Then, the SWCNH solution was sprayed and sintered at 500 °C; this acted as a second electrode for the supercapacitor. A separator consisting of a Surlyn sheet was placed between the two supercapacitor electrodes, and a liquid electrolyte of $EMIBF_4$ was filled and gently sealed. Figure 2 presents the resultant photocapacitor (integrated the dye sensitized solar cell with the supercapacitor).

3. CHARACTERIZATION AND MEASUREMENTS

Microstructural studies of carbon, SWCNH, and SWCNH decorated carbon bilayer films and cross sections are examined by SEM (scanning electron microscopy, JEOL, JSM-IT500) and also by EDAX through APEX. X-ray diffraction studies

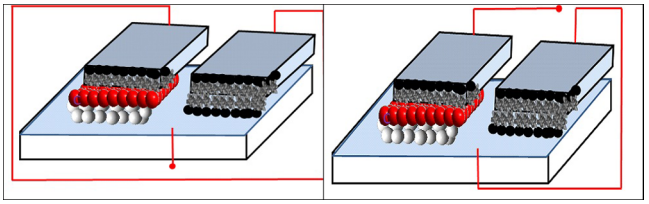

Figure 2. Photo supercapacitor connections under illumination and in the dark.

were recorded by a Rigaku Miniflex diffractometer in between 0° and 80° of 2θ value. Electrocatalytic activity was observed through cyclic voltammetry (CV) with an electrochemical workstation CompactSTAT.h IVIUM technology with three-electrode configurations. Ag/Ag^+ was used as the reference electrode, by use of acetonitrile solution containing 0.5 mM I_2, 0.1 M $LiClO_4$, and 5 mM LiI, at a scan rate of 50 mV s^{-1}. Photocurrent density (J)−voltage (V) characterization of the developed test devices was examined with a solar simulator (PEC-L01, Peccell Inc.) containing a spectral filter (AM 1.5) and source meter (2401N Keithley). The light intensity of the solar simulator is adjusted to 100 mW/cm^2. The Tafel polarization plots and EIS (electrochemical impedance spectroscopy) were carried out for symmetrical dummy test cells (CompactSTAT.h workstation), with 10 mV of amplitude between frequencies of 1 Hz and 1 MHz.

4. RESULTS AND DISCUSSION

The microstructural studies of carbon, SWCNH, and SWCNH decorated carbon based electrodes are examined by SEM studies, and the resulting images are presented as Figure 3. The

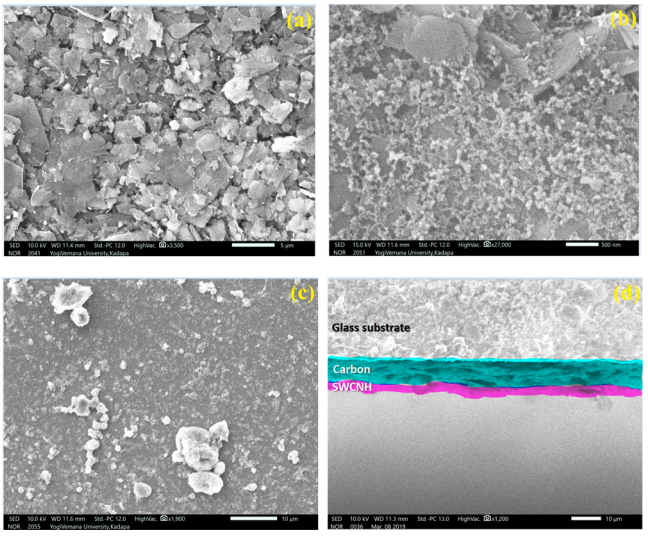

Figure 3. SEM images of (a) carbon, (b) SWCNH/carbon, (c) SWCNH, and (d) cross-sectional view of SWCNH/carbon.

pristine carbon had flakes of smooth and thin layer structures shown in Figure 3a. Figure 3b represents a SWCNH/carbon based electrode having an interconnected nature. Carbon flakes covering the SWCNH layer are observed for the SWCNH coated carbon electrode, shown in Figure 3b. Figure 3c presents the SWCNH coated electrode, consisting of agglomerated SWCNHs. Figure 3d represents the cross-sectional view of SWCNH over carbon coated electrodes. The carbon film thickness of 12 μm is present, over which a

https://doi.org/10.1021/acsaem.1c02087
ACS Appl. Energy Mater. 2021, 4, 11225−11233

thin SWCNH layer is observed. The EDAX spectra are represented in Supporting Information Figure S1. The X-ray diffraction (XRD) studies are performed and presented as Figure S2 of Supporting Information.

The performance of the electrocatalytic activity of the developed counter electrodes is monitored in an I^-/I_3^- redox based solution by use of cyclic voltammetry (CV) studies having a three-electrode configuration. The platinum (Pt) wire acts as the counter electrode, and the Ag/Ag^+ acts as the reference electrode in acetonitrile based solution consisting of 10 mM LiI, 0.1 M $LiClO_4$, and 1 mM I_2.

The prepared working electrodes (carbon, SWCNH, SWCNH/carbon, and Pt solution coated FTO glass substrates) are inserted into the solution, and ultrapure N_2 (nitrogen) gas is purged well before the start of the scans for better performance. The witnessed results are presented in Figure 4, in which the two pairs of prominent of peaks are

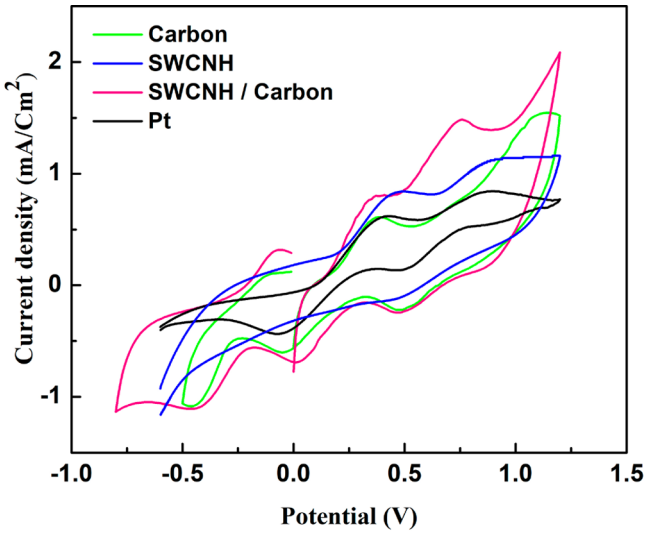

Figure 4. *C*−*V* curves of carbon, SWCNH, SWCNH/carbon, and Pt electrodes.

clearly observed. The two pairs of redox peaks, anodic peaks and cathodic peaks, are observed for carbon, SWCNH/carbon, Pt, and SWCNH. The cathodic peak reflects the reduction of tri-iodide, and anodic peaks reflect the oxidation of iodide and tri-iodide. SWCNH/carbon presented oxidation and reduction peaks similar to those for Pt. This specifies that the SWCNH/carbon electrode displays improved catalytic activity compared with that of Pt. The redox reaction that occurs at the CE of DSSC in the cyclic voltammogram is owed to the reduction of iodine molecules. The SWCNH/carbon electrode presented both higher oxidation and reduction current density in a comparison with those of Pt, predicting a wild rate of triiodide reduction.[38] For the carbon working electrode, there is another pair of peaks found; this is associated with oxidation and reduction of carbon itself.[39]

The Tafel slope is an intrinsic characteristic of electrocatalyst materials that is determined by the rate-limiting step.[40] Figure 5 represents Tafel polarization curves with logarithmic current density (log mA) as a voltage function for oxidation and reduction reactions of carbon, SWCNH/carbon, SWCNH, and Pt electrodes. Tafel polarization was accomplished with symmetric dummy test cells (two similar counter electrodes sandwiched, with filled electrolyte into the cell to become

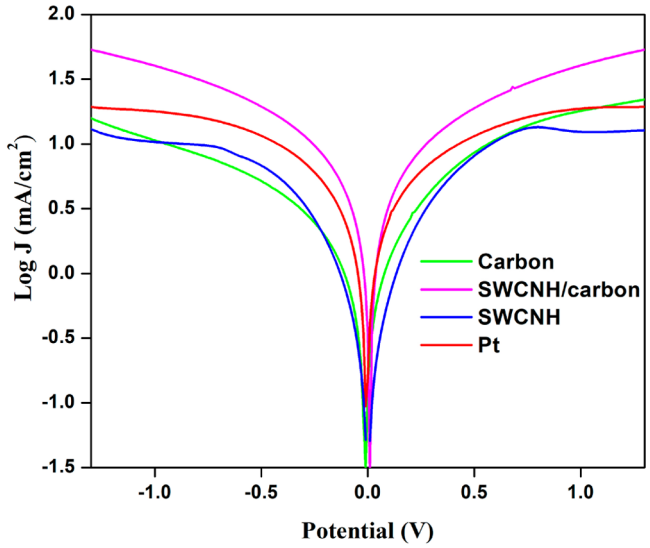

Figure 5. Tafel polarization curves of carbon, SWCNH, SWCNH/carbon, and Pt CEs.

symmetric dummy test cells). From Figure 5, the SWCNH/carbon electrode performed a larger exchange current density (J_O) than the carbon, SWCNH, which implies a higher electrocatalytic activity and reduced charge-transfer resistance at the electrode−electrolyte interface. Tafel curve branches of anodic and cathodic nature for the SWCNH/carbon electrode presented a greater slope representing a higher exchange current density.

Figure 6 depicts photo current density−voltage (*J*−*V*) curves; its resultant photovoltaic parameter values with

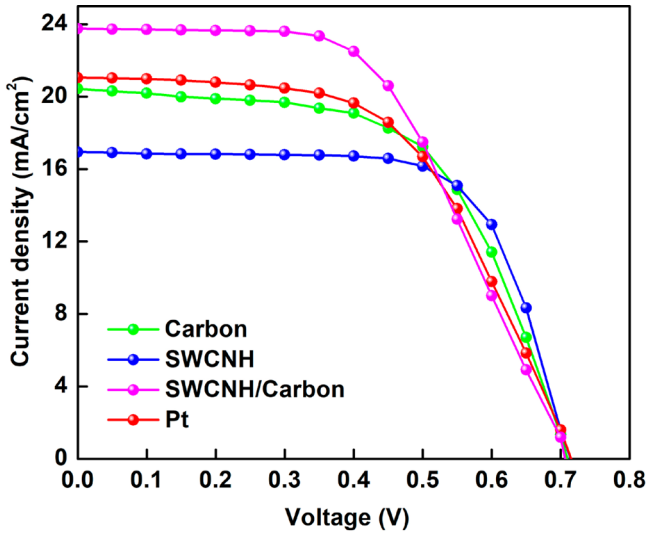

Figure 6. *I*−*V* curves of carbon, SWCNH/carbon, SWCNH, and Pt CE based DSSCs.

acetonitrile based electrolyte are given in Table 1. The photovoltaic performance with N719 dye based DSSC accumulated with prepared electrodes and derived performance of photovoltaic parameters, like short-circuit current density, efficiency, fill factor, open-circuit voltage, is tabulated in Table 1. DSSC with carbon CE shows J_{sc} = 20.44 mA/cm^2; V_{oc} is 0.71 V, with a fill factor of 0.63, yielding a PCE of 9.14%. In contrast, the cell that ended with SWCNH/carbon

https://doi.org/10.1021/acsaem.1c02087
ACS Appl. Energy Mater. 2021, 4, 11225−11233

Table 1. Fabricated DSSC Photovoltaic Parameters

parameter	carbon	SWCNH	SWCNH/carbon	Pt
V_{oc} (V)[a]	0.71	0.72	0.72	0.71
J_{sc} (mA/cm^2)[a]	20.44	16.99	23.76	21.04
fill factor (FF)[a]	0.63	0.63	0.65	0.63
efficiency (η) (%)[a]	9.14	7.74	11.12	9.41

[a]V_{oc}: ±30 mV. J_{sc}: ±0.20 mA/cm^2. FF: ±0.03. η: ±0.10.

harvested η = 11.12% with V_{oc} = 0.72 V, J_{sc} = 23.76 mA/cm^2, and FF = 0.65. For comparison, SWCNH and Pt based test cells are fabricated, and their photovoltaic parameters are tabulated in Table 1.

The overall performance of the SWCNH/carbon based DSSC is high due to the conductivity of carbon and the high electrochemical activity of SWCNH; the composite DSSC exhibited a higher PCE. The stability of the materials and device performance are provided in the Supporting Information, Figure S3a,b.

EIS (electrochemical impedance spectroscopy) measurements were performed to examine the interfacial charge-transfer process that occurs at the electrode−electrolyte−electrode interfaces of symmetrical dummy test cells. The Nyquist plots consist of two semicircles as shown in Figure 7.

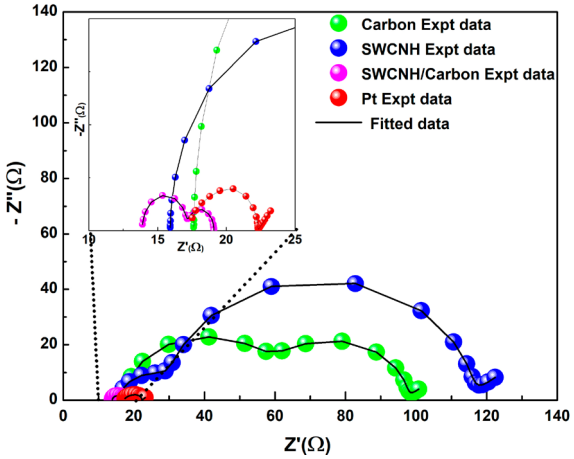

Figure 7. EIS of dummy test cells made with the same CEs.

At the higher-frequency region, the first semicircle intercept on the real axis is assigned to series resistance (R_S) of the FTO−SWCNH/carbon interface, whereas, at the lower-frequency range, the intercept on the real axis signifies R_{CT} (charge-transfer resistance). The R_S and R_{CT} values are evaluated through the fitted equivalent circuit (inset of Figure 7), tabulated in Table 2.

From this, we can conclude that SWCNH/carbon offers a better performance. The R_{CT} value depends on the counter electrode's catalytic materials; the fitted R_{CT} for the SWCNH/carbon CE is effective compared to that of the Pt CE; the higher value R_{CT} of SWCNH/carbon indicates a higher ability for the reduction of I_3^- to I^- in an electrolyte solution compared with that of the Pt CE.

Table 2. EIS Parameters and J_O of Dummy Test Cells Fabricated with the Same CEs

parameter	SWCNH	carbon	SWCNH/carbon	Pt
Rs	15.92	17.60	13.81	17.41
R_{CT}	21.01	37.90	19.40	19.68
J_O (mA/cm^2)	1.50	3.77	10.43	8.75

The Bode phase plots are presented as Figure 8; from the peak values, the electron lifetime (τ_e) is evaluated for carbon,

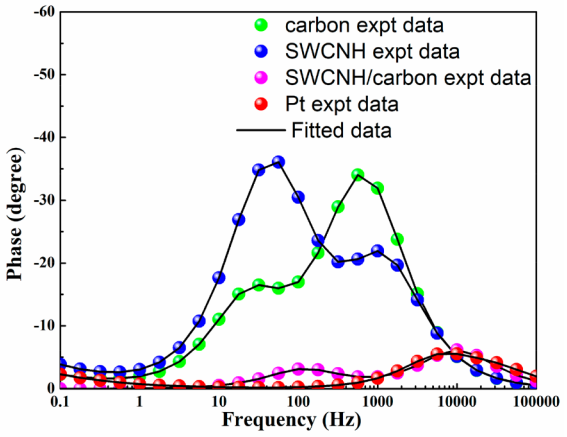

Figure 8. Symmetric dummy cell Bode phase plots.

SWCNH, SWCNH/carbon, and Pt based devices. Here, the frequency peaks confirm the charge transfer at different interfaces for these devices. The SWCNH/carbon test device's characteristic peak frequency is present at the lower-frequency side, demonstrating a longer electron lifetime of 1.3 ms, which is evaluated by using the equation $\tau_e = 1/2\pi f_{max}$.

Bifacial DSSM Performance. Dye sensitized solar cells are potentially useful as photovoltaic technology for indoor as well as outdoor applications. In particular, a bifacial DSSC is a promising candidate for oriented building integrated photovoltaics (BIPVs), which enables harvesting both direct sunlight and diffused light (indoor light) for power conversion. The present work demonstrated a W-type module which consists of six individual DSSC test cells in a connected series, named DSSM; the potential for power conversion of sunlight and indoor light is illustrated in Figure 9.

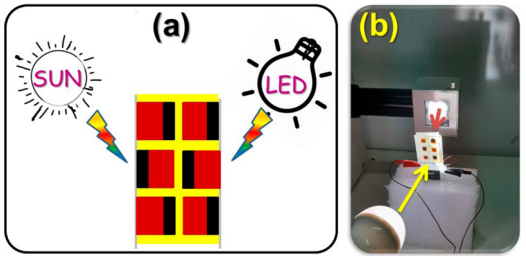

Figure 9. Developed W-type DSSM module taking advantage of both (a) sunlight and (b) indoor light conversion.

The developed bifacial DSSM was exposed to light power of 100 mW/cm^2 in addition to indoor light of 1000 lx; the performance is measured, and the obtained results of $J-V$ characteristic performance are depicted in Figure 10. Photovoltaic parameters are summarized in Table 3. Here, the DSSM part exists in the W-type design in which photoelectrodes interchange between the front side and the back side of the submodule as represented in Figure 1. The DSSM revealed a

https://doi.org/10.1021/acsaem.1c02087
ACS Appl. Energy Mater. 2021, 4, 11225−11233

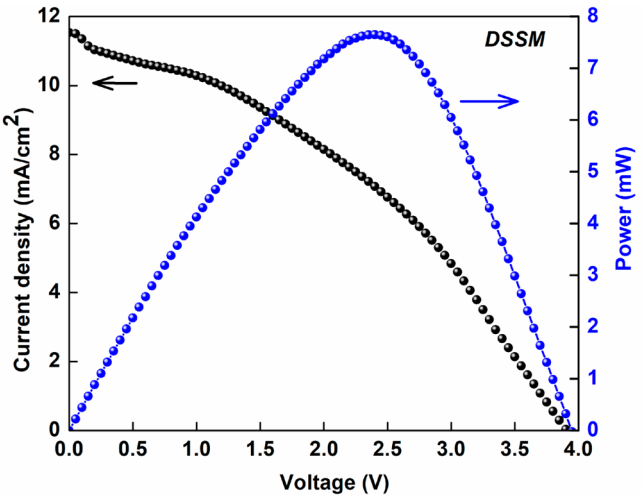

Figure 10. *J*–*P*–*V* plot of fabricated dye sensitized solar module.

Table 3. Photovoltaic Parameters of DSSM

parameter	DSSM
V_{oc} (V)	3.94
J_{sc} (mA/cm^2)	11.53
fill factor	0.53
efficiency (η) (%)	19.71

V_{OC} of 3.94 V, J_{SC} of 11.53 mA/cm^2, and FF of 0.53, which leads to a PCE (power conversion efficiency) of 19.71%.

Figure 10 also presents the power–voltage characteristic of bifacial DSSM. Here, particular attention has to be paid to the shape of the curve, since that can provide precious information about the photocharging process. The power has a maximum value at 2.4 V. As reported, the overall efficiency increases quickly in the first part of the photocharge, since the storage of energy increases almost linearly in this region.

Supercapacitor Performance. The performance of the fabricated supercapacitor using SWCNH/carbon is made through cyclic voltammetry, EIS, and galvanostatic charge–discharge (GCD) measurements. The supercapacitor is loaded with efficient electrolyte. Cyclic voltammetry plots are recorded from 10 to 200 mV s^{-1} scan rates over a voltage window from 0 to 1.5 V, and the results are shown in Figure 11a. The obtained curves are in a quasirectangular shape. From CV, the SWCNH/carbon based SC encircles a larger area, which indicates superior capacitance performance. The GCD plots are measured in the range of current densities from 0.5 to 1.5 mA/cm^2 over the voltage window from 0 to 1 V (Figure 11b), which is shown in a nearly triangular shape. Areal capacitance (ASC), power density (P), and energy density (E) in the two-electrode mode are evaluated by using the equations mentioned below, and the evaluated parameter values are tabulated in Table 4.

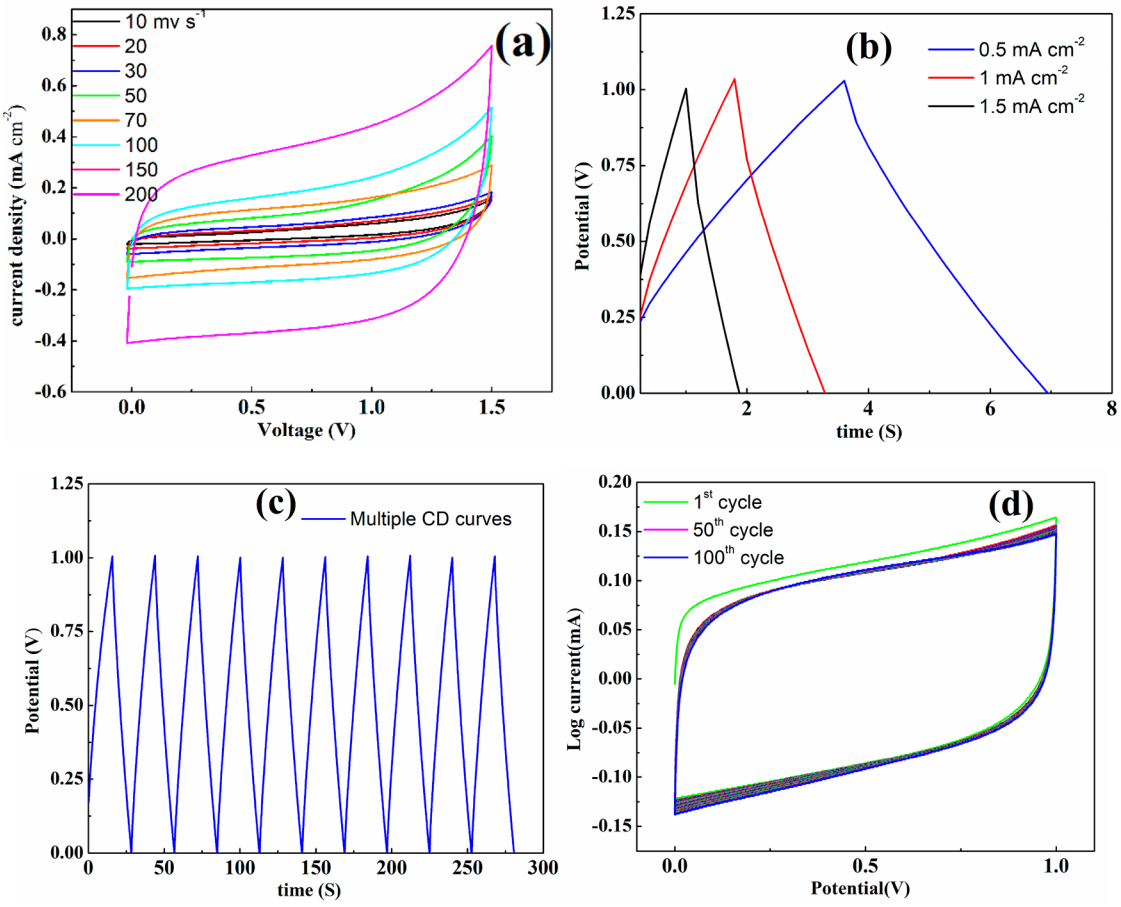

Figure 11. (a) CD curves of SWCNH/carbon SC at different charge–discharge current densities. (b) CV curves of the SC from 10 mV s^{-1} to 200 mV s^{-1} scan rates. (c) Galvanostatic charging and discharging curves versus time plot. (d) 100 cycles of CV curves at a scan rate of 100 mV s^{-1}.

https://doi.org/10.1021/acsaem.1c02087
ACS Appl. Energy Mater. 2021, 4, 11225–11233

$$\text{ASC (F g}^{-1}) = (I \times \Delta t)/m \times \Delta V$$

$$E\ (\text{Wh kg}^{-1}) = 0.5 \times \text{ASC} \times \Delta V^2$$

$$P\ (\text{W kg}^{-1}) = E/\Delta t$$

Table 4. Electrochemical Properties of Symmetric Supercapacitors

current density, I (mA/cm^2)	ASC (F g^{-1})	E (Wh kg^{-1})	P (W kg^{-1})
0.5	74.27	38.16	6.51
1.0	72.21	37.43	13.72
1.5	64.19	35.48	19.71

In the above equations, the current density is I in mA/cm^2, the discharge time is Δt in s, and the voltage window ΔV is in V. From a decrease in current density from 1.5 to 0.5 mA/cm^2, the discharge time is increased, which confirms that the charge storing capacity of the developed material is higher owing to the accessibility of a greater number of active sites which are electrochemically available and have a lower charge-transfer resistance. The SWCNH/carbon electrode galvanostatic charge−discharge performance up to 10 cycles for voltage starting from 0 to 1 V is demonstrated in Figure 11c, and the obtained curves have a triangular-like shape. The areal specific capacitance (ASC), energy density (E), and power density (P) are evaluated, with the values of 74.27 F g^{-1}, 38.16 Wh kg^{-1}, and 6.51 W kg^{-1}, respectively, by applying a current density of 0.5 mA/cm^2. The SWCNH/carbon electrode is higher in electrical conductivity, with greater electrocatalytic active surface sites which improve the overall storage of charge (Figure 11b). Figure 11d shows that the CV is constant during 100 cycles of measurement, evidencing stable performance.

An electrochemical impedance spectroscopy measurement for SC is also performed, and the results are depicted in Figure 12. At the higher-frequency side, the series resistance value found as R_S is 33.98 Ω for the SWCNH/carbon based supercapacitor in $EMIBF_4$ based acetonitrile electrolyte.

DSSM Working Demonstration through an Electronic LED. The DSSM delivered a higher power conversion efficiency (η) of 19.71% and the energy density of the most of reported studies.[20,41−43] By considering the advantage of this as well as bifacial illumination of the 100 mW/cm^2 light condition at one side, and the indoor light of 1000 lx on the other side, DSSM which demonstrated an open-circuit voltage of 3.94 V (experimental setup shown in Figure 13) is adequate

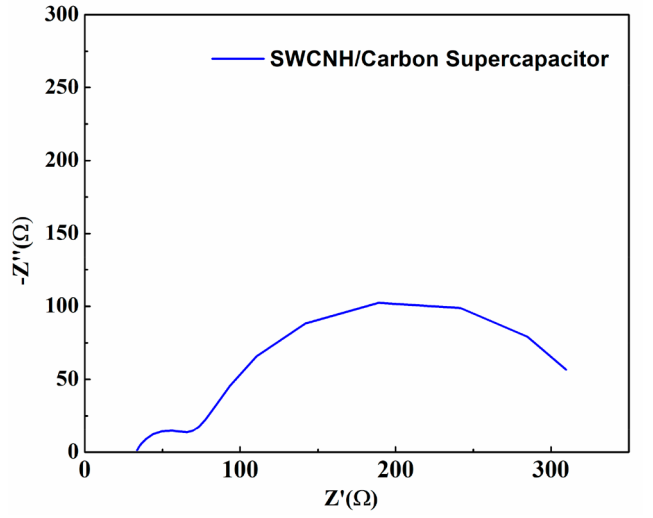

Figure 12. Electrochemical impedance spectroscopy of supercapacitor.

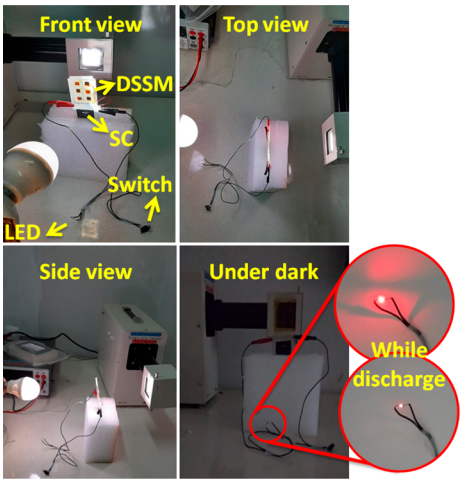

Figure 13. DSSM illumination from both sides, under dark condition discharge of SC lighting an LED.

to charge the supercapacitor. With the discharge of SC, it lit up a light emitting diode (LED) which is shown as an inset for Figure 13, demonstrating its potential as a power source. This is suggesting the better electrochemical features for the SWCNH/carbon device. Figure 13 evidenced lighting of the LED by the supercapacitor under dark conditions.

The overall photoconversion and storage efficiency ($\eta_{overall}$) of the photocapacitor (PC) device are calculated by use of the following equations.

$$\eta_{overall} = (E_{PC} \times A_{SC})/(E_{light} \times t_{ch} \times A_{DSSC})$$

In the above equation, E_{PC} is the energy density of PC, E_{light} is the incident light power density (100 mW/cm^2), t_{ch} is the photocharging time, A_{SC} is the effective active surface area of supercapacitor part, and A_{DSSC} is the effective active surface area of the solar cell part in PC.

The energy storage efficiency of the PC is given by the following equation.

$$\eta_{storage} = \eta_{overall}/\eta_{conversion}$$

In the above equation, $\eta_{storage}$ is the energy storage efficiency of the supercapacitor part in the PC, and $\eta_{conversion}$ is the PCE of solar cell in the PC (19.71%). Thus, $\eta_{overall}$ and $\eta_{storage}$ of the PC device are determined to be 10.46% and 53.3%, respectively.

5. CONCLUSIONS

The photovoltaic performance of a single wall carbon nanohorn (SWCNH) assisted carbon counter electrode (CE) based DSSC demonstrated a power conversion efficiency (PCE) of 11.12%, which is a motivation to develop a submodule (DSSM) which consists of six DSSCs connected in series. This setup acted as a bifacial module. This notable performance drove the fabrication of a SWCNH/carbon based photocapacitor, which exhibited excellent performance and

https://doi.org/10.1021/acsaem.1c02087
ACS Appl. Energy Mater. 2021, 4, 11225−11233

demonstrated an electronic light emitting device (LED) function upon discharge of the SC. The DSSM is capable of converting light illuminated from both sides into electric power, which showed a remarkable power conversion efficiency of 19.71% and an open-circuit voltage of 3.94 V; this reflects the potential for building integrated photovoltaics (BIPVs).

■ ASSOCIATED CONTENT

Supporting Information

The Supporting Information is available free of charge at https://pubs.acs.org/doi/10.1021/acsaem.1c02087.

EDAX, XRD, and details about the stability of the materials and test devices (PDF)

■ AUTHOR INFORMATION

Corresponding Author

Raghavender Mitty − *Department of Physics, Yogi Vemana University, Kadapa 516005, India;* orcid.org/0000-0002-0958-4378; Email: toraghavender@rediffmail.com

Authors

Gurulakshmi Maddala − *Department of Physics, Yogi Vemana University, Kadapa 516005, India*

Meenakshamma Ambapuram − *Department of Physics, Yogi Vemana University, Kadapa 516005, India*

VijayaLaxmi Tankasala − *Department of Mathematics, N.T.R. Government Degree College for Women, Mahabubnagar 509001, India*

Complete contact information is available at: https://pubs.acs.org/10.1021/acsaem.1c02087

Notes

The authors declare no competing financial interest.

■ ACKNOWLEDGMENTS

G.M. is thankful to the Department of Science and Technology (DST)-INSPIRE for financial support through IF 160564. R.M. thanks DST-SERB (EMR/CRG) EMR/2016/007049 for the utilized equipment purchased through this financial support. A.M. is thankul to DST for WOS-B through DST/WOS-B/ER-7/2021.

■ REFERENCES

(1) Hagfeldt, A.; Boschloo, G.; Sun, L.; Kloo, L.; Pettersson, H. Dye Sensitized Solar Cells. *Chem. Rev.* **2010**, *110*, 6595−6663.

(2) Li, L. L.; Diau, E. W.G. Porphyrin-Sensitized Solar Cells. *Chem. Soc. Rev.* **2013**, *42*, 291−304.

(3) Yella, A.; Lee, H. W.; Tsao, H. N.; Yi, C. Y.; Chandiran, A. K.; Nazeeruddin, M. K.; Diau, E. W. G.; Yeh, C. Y.; Zakeeruddin, S. M.; Gratzel, M. Porphyrin-Sensitized Solar Cells with Cobalt (II/III) Based Redox Electrolyte Exceed 12% Efficiency. *Science* **2011**, *334*, 629−634.

(4) Ito, S.; Murakami, T. N.; Comte, P.; Liska, P.; Grätzel, C.; Nazeeruddin, M. K.; Grätzel, M. Fabrication of thin film dye sensitized solar cells with solar to electric power conversion efficiency over 10%. *Thin Solid Films* **2008**, *516*, 4613−4619.

(5) Gao, F.; Wang, Y.; Shi, D.; Zhang, J.; Wang, M.; Jing, X.; Humphry-Baker, R.; Wang, P.; Zakeeruddin, S. M.; Grätzel, M. Enhance the Optical Absorptivity of Nanocrystalline TiO2 Film with High Molar Extinction Coefficient Ruthenium Sensitizers for High Performance Dye-Sensitized Solar Cells. *J. Am. Chem. Soc.* **2008**, *130*, 10720−10728.

(6) Du, Y. F.; Fan, J. Q.; Zhou, W. H.; Zhou, Z. J.; Jiao, J.; Wu, S. X. One-Step Synthesis of Stoichiometric $Cu_2ZnSnSe_4$ as Counter Electrode for Dye-Sensitized Solar Cells. *ACS Appl. Mater. Interfaces* **2012**, *4*, 1796−1802.

(7) Gong, F.; Wang, H.; Xu, X.; Zhou, G.; Wang, Z. S. In Situ Growth of $Co_{0.85}Se$ and $Ni_{0.85}Se$ on Conductive Substrates as high-performance Counter Electrodes for Dye-Sensitized Solar Cells. *J. Am. Chem. Soc.* **2012**, *134*, 10953−10958.

(8) Wang, M.; Anghel, A. M.; Marsan, B. t.; Cevey Ha, N. L.; Pootrakulchote, N.; Zakeeruddin, S. M.; Grätzel, M. CoS Supersedes Pt as Efficient Electrocatalyst for Triiodide Reduction in Dye Sensitized Solar Cells. *J. Am. Chem. Soc.* **2009**, *131*, 15976−15977.

(9) Wu, M.; Lin, X.; Wang, Y.; Wang, L.; Guo, W.; Qi, D.; Peng, X.; Hagfeldt, A.; Grätzel, M.; Ma, T. Economical Pt-Free Catalysts for Counter Electrodes of Dye-Sensitized Solar Cells. *J. Am. Chem. Soc.* **2012**, *134*, 3419−3428.

(10) Roy-Mayhew, J. D.; Bozym, D. J.; Punckt, C.; Aksay, I. A. Functionalized Graphene as a Catalytic Counter Electrode in Dye Sensitized Solar Cells. *ACS Nano* **2010**, *4*, 6203−6211.

(11) Li, G. R.; Song, J.; Pan, G. L.; Gao, X. P. Highly Pt-like Electrocatalytic Activity of Transition Metal Nitrides for Dye Sensitized Solar Cells. *Energy Environ. Sci.* **2011**, *4*, 1680−1683.

(12) Wu, M. X.; Lin, X. A.; Hagfeldt, A.; Ma, T. L. Low-Cost Molybdenum Carbide and Tungsten Carbide Counter Electrodes for Dye-Sensitized Solar Cells. *Angew. Chem., Int. Ed.* **2011**, *50*, 3520−3524.

(13) Jiang, Q. W.; Li, G. R.; Gao, X. P. Highly ordered TiN nanotube arrays as counter electrodes for dye-sensitized solar cells. *Chem. Commun.* **2009**, *44*, 6720−6722.

(14) Imoto, K.; Takahashi, K.; Yamaguchi, T.; Komura, T.; Nakamura, J.; Murata, K. High-Performance Carbon Counter Electrode for Dye-Sensitized Solar Cells. *Sol. Energy Mater. Sol. Cells* **2003**, *79*, 459−469.

(15) Murakami, T. N.; Ito, S.; Wang, Q.; Nazeeruddin, M. K.; Bessho, T.; Cesar, I.; Liska, P.; Humphry-Baker, R.; Comte, P.; Pechy, P.; Grätzel, M. Highly Efficient Dye-Sensitized Solar Cells Based on Carbon Black Counter Electrodes. *J. Electrochem. Soc.* **2006**, *153*, A2255−A2261.

(16) Ramasamy, E.; Lee, W. J.; Lee, D. Y.; Song, J. S. Nanocarbon Counter electrode for Dye Sensitized Solar Cells. *Appl. Phys. Lett.* **2007**, *90*, 173103.

(17) Huang, Z.; Liu, X. H.; Li, K. X.; Li, D. M.; Luo, Y. H.; Li, H.; Song, W. B.; Chen, L. Q.; Meng, Q. B. Application of Carbon Materials as Counter Electrodes of Dye-Sensitized Solar Cells. *Electrochem. Commun.* **2007**, *9*, 596−598.

(18) Suzuki, K.; Yamaguchi, M.; Kumagai, M.; Yanagida, S. Application of Carbon Nanotubes to Counter Electrodes of Dye-Sensitized Solar Cells. *Chem. Lett.* **2003**, *32*, 28−29.

(19) Hino, T.; Ogawa, Y.; Kuramoto, N. Preparation of Functionalized and Non-functionalized Fullerene Thin Films on ITO Glasses and the Application to a Counter Electrode in a Dye-Sensitized Solar Cell. *Carbon* **2006**, *44*, 880−887.

(20) Das, A.; Ojha, M.; Subramanyam, P.; Deepa, M. A poly (3,4-propylene dioxy thiophene)/carbon micro-sphere-bismuth nanoflake composite and multifunctional Co-doped graphene for a benchmark photo-supercapacitor. *Nanoscale Adv.* **2020**, *2*, 2925−2942.

(21) Ebbesen, T. W.; Lezec, H. J.; Hiura, H.; Bennett, J. W.; Ghaemi, H. F.; Thio, T. Electrical Conductivity of Individual Carbon Nanotubes. *Nature* **1996**, *382*, 54−56.

(22) Chew, S. Y.; Ng, S. H.; Wang, J. Z.; Novak, P.; Krumeich, F.; Chou, S. L.; Chen, J.; Liu, H. K. Flexible Free-Standing Carbon Nanotube Films for Model Lithium-Ion Batteries. *Carbon* **2009**, *47*, 2976−2983.

(23) Chen, Y. S.; Huang, J. H.; Chuang, C. C. Glucose Biosensor Based on Multiwalled Carbon Nanotubes Grown Directly on Si. *Carbon* **2009**, *47*, 3106−3112.

(24) Gurulakshmi, M.; Meenakshamma, A.; Susmitha, K.; Charanadhar, N.; Srikanth, V. V. S. S.; Narendra Babu, S.; Venkata Subbaiah, Y. P.; Venkateswarlu, Katta; Raghavender, M. A transparent

and Pt-free all-carbon nanocomposite counter electrode catalyst for efficient dye sensitized solar cells. *Sol. Energy* **2019**, *193*, 568−575.
(25) Gurulakshmi, M.; Meenakshamma, A.; Susmitha, K.; Venkata Subbaiah, Y.; Raghavender, M. Enhanced Performance of Dye-Sensitized Solar Cells (DSSCs) Based on MoS_2/Single-Walled Carbon Nanohorns Electrochemically Deposited Bilayer Counter Electrodes. *ChemPlusChem* **2020**, *85*, 2599−2605.
(26) Lodermeyer, F.; Costa, R. D.; Guldi, D. M. Review—Single-Walled Carbon Nanohorn-Based Dye-Sensitized Solar Cells. *ECS J. Solid State Sci. Technol.* **2017**, *6*, M3140−M3147.
(27) Huaulmé, Q.; Mwalukuku, V. M.; Joly, D.; Liotier, J.; Kervella, Y.; Maldivi, P.; Narbey, S.; Oswald, F.; Riquelme, A. J.; Anta, J. A.; Demadrille, R. Photochromic Dye-Sensitized Solar Cells with Light-Driven Adjustable Optical Transmission and Power Conversion Efficiency. *Nat. Energy* **2020**, *5*, 468−477.
(28) Zhang, K.; Qin, C.; Yang, X.; Islam, A.; Zhang, S.; Chen, H.; Han, L. High-Performance, Transparent, Dye-Sensitized Solar Cells for See-through Photovoltaic Windows. *Adv. Energy Mater.* **2014**, *4*, 1301966.
(29) Gokul, G.; Pradhan, S. C.; Soman, S. Dye-Sensitized Solar Cells as Potential Candidate for Indoor/Diffused Light Harvesting Applications: From BIPV to Self-Powered IoTs. *Advances in Solar Energy Research*; Springer: Singapore, 2019; pp 281−316. DOI: 10.1007/978-981-13-3302-6_9
(30) Fakharuddin, A.; Jose, R.; Brown, T. M.; Fabregat-Santiago, F.; Bisquert, J. A Perspective on the Production of Dye-Sensitized Solar Modules. *Energy Environ. Sci.* **2014**, *7*, 3952−3981.
(31) Michaels, H.; Rinderle, M.; Freitag, R.; Benesperi, I.; Edvinsson, T.; Socher, R.; Gagliardi, A.; Freitag, M. Dye-Sensitized Solar Cells under Ambient Light Powering Machine Learning: Towards Autonomous Smart Sensors for Internet of Things. *Chem. Sci.* **2020**, *11*, 2895−2906.
(32) Zhang, W.; Wu, Y.; Bahng, H. W.; Cao, Y.; Yi, C.; Saygili, Y.; Luo, J.; Liu, Y.; Kavan, L.; Moser, J.-E.; Hagfeldt, A.; Tian, H.; Zakeeruddin, S. M.; Zhu, W.-H.; Grätzel, M. Comprehensive Control of Voltage Loss Enables 11.7% Efficient Solid-State Dye-Sensitized Solar Cells. *Energy Environ. Sci.* **2018**, *11*, 1779−1787.
(33) Cao, Y.; Liu, Y.; Zakeeruddin, S. M.; Hagfeldt, A.; Grätzel, M. Direct Contact of Selective Charge Extraction Layers Enables High-Efficiency Molecular Photovoltaics. *Joule* **2018**, *2*, 1108−1117.
(34) Freitag, M.; Teuscher, J.; Saygili, Y.; Zhang, X.; Giordano, F.; Liska, P.; Hua, J.; Zakeeruddin, S. M.; Moser, J. E.; Grätzel, M.; Hagfeldt, A. Dye-Sensitized Solar Cells for Efficient Power Generation under Ambient Lighting. *Nat. Photonics* **2017**, *11*, 372−378.
(35) Vega Garita, V.; Ramirez Elizondo, L.; Narayan, N.; Bauer, P. Integrating a photovoltaic storage system in one device: A critical review. *Prog. Photovoltaics* **2018**, *27*, 346 DOI: 10.1002/pip.3093.
(36) Ramadoss, A.; Saravanakumar, B.; Kim, S.-J. *Fabrication and Characterization of Supercapacitors toward Self-Powered System*; IntechOpen: London, 2018; pp 167−192. DOI: 10.5772/intechopen.73647
(37) Yuan, L.; Xiao, X.; Ding, T.; Zhong, J.; Zhang, X.; Shen, Y.; Hu, B.; Huang, Y.; Zhou, J.; Wang, Z. L. Paper-Based Supercapacitors for Self-Powered Nanosystems. *Angew. Chem., Int. Ed.* **2012**, *51*, 4934−4938.
(38) Hong, C. K.; Ko, H. S.; Han, E. M.; Park, K. H. Electrochemical Properties of Electrodeposited PEDOT Counter Electrode for Dye-sensitized Solar Cells. *Int. J. Electrochem. Sci.* **2015**, *10*, 5521−5529.
(39) Costa, C.; Mesquita, I.; Andrade, L.; Mendes, A. Photo-electrochromic devices: Influence of device architecture and electrolyte composition. *Electrochim. Acta* **2016**, *219*, 99−106.
(40) He, J.; Lee, L. T. L.; Yang, S.; Li, Q.; Xiao, X.; Chen, T. Printable Highly Catalytic Pt- and TCO-Free Counter Electrode for Dye-Sensitized Solar Cells. *ACS Appl. Mater. Interfaces* **2014**, *6*, 2224−2229.
(41) Scalia, A.; Varzi, A.; Lamberti, A.; Tresso, E.; Jeong, S.; Jacob, T.; Passerini, S. High energy and high voltage integrated photo-electrochemical double layer capacitor. *Sustainable Energy Fuels* **2018**, *2*, 968−977.
(42) Gao, K.; Ti, D.; Zhang, Z. A photocapacitor with high working voltage and energy density. *Sustainable Energy Fuels* **2019**, *3*, 1937−1942.
(43) Sasidharan, S.; Pradhan, S. C.; Jagadeesh, A.; Nair, B. N.; Mohamed, A. A. P.; K. N, N. U.; Soman, S.; Hareesh, U. N. S. Bifacial Dye-Sensitized Solar Cells with Enhanced Light Scattering and Improved Power Conversion Efficiency under Full Sun and Indoor Light Conditions. *ACS Appl. Energy Mater.* **2020**, *3*, 12584−12595.

ISBN: 978-81-947958-3-4

، آمینہ بیگم
، ریسرچ اسکالر
، محکمہ تاریخ
، مولانا آزاد قومی اردو یونیورسٹی
حیدرآباد۔
amenabegum.s777@gmail.com

سلطنت آصفیہ کے امیر پائیگاہ سرآسمان جاہ کی رعایا پروری

آمینہ بیگم (ریسرچ اسکالر، شعبۂ تاریخ)
مولانا آزاد نیشنل اردو یونیورسٹی، گچی بولی، حیدرآباد

سلطنت آصفیہ جنوبی ہند کی ایک منفرد نظام سلطنت گزری ہے۔ یہ سلطنت نہ صرف ہندوستان بلکہ عالمی سطح پر منفرد مقام رکھتی ہے۔ میر قمرالدین خاں نے 1724ء میں سلطنت آصفیہ کی بنیاد ڈالی۔ جس میں 7 فرمانروا گزرے ہیں۔ اورنگ آباد اکا پہلا دارالخلافہ تھا۔ لیکن بعد میں نظام علی خاں نے حیدرآباد کو اپنا دارالخلافہ بنایا۔

سلطنت آصفیہ میں امرائے پائیگاہ کا مقام و مرتبہ حکمران وقت کے بعد کا تھا۔ یہ نائب سلطنت ہوا کرتے تھے۔ ابوالفتح خاں سے پائیگاہی امارت قائم ہوئی۔ سلطنت کا تحفظ، سازشوں، بغاوتوں کی سرکوبی اور دیوان اور منصب داروں پر کنٹرول کرنا ان کا اہم مقصد تھا۔ یہ صرف نظام کے آگے جوابدہ تھے۔ یہ اپنے علاقے میں خودمختار تھے۔

نواب سرآسمان جاہ کا نام محمد مظفرالدین خاں تھا۔ آپ سلطان الدین خاں کے چھوٹے بیٹے تھے۔ آپ کی شادی سلطنت آصفیہ کے پانچویں حکمراں افضل الدولہ کی دختر اور میر محبوب علی خاں کی ہمشیرہ پرنس انساء بیگم سے ہوئی۔ آپ کو اردو، عربی، فارسی، انگریزی زبان پر عبور حاصل تھا۔ سلطنت آصفیہ میں صدر المہامی عدالت کے جلیل القدر عہدے پر فائز ہوئے۔ انہوں نے باوقار اپنے خدمات انجام دیے۔ انہوں نے اپنے دور صدارالمہامی میں رعایا کی فلاح و بہبودی، ان کے بنیادی ضرورتوں کی تکمیل کو اپنا نصب العین سمجھتے تھے۔ ان کے چند اہم کارنامے اس طرح ہیں۔

تعلیم یافتگان کی بازآبادکاری تک نصف تنخواہ جاری کرتے ہوئے ان کی بازآبادکاری کو یقینی بنایا۔ اس سے کئی خاندانوں کی کفالت ہوئی۔ غریب محتاج خواہشمند حجاج کے لیے مفت حج کی سہولت فراہم کیے۔ 1893ء میں زلزلہ باری سے تباہ شدہ مکانات کی دوبارہ تعمیر، بازآبادکاری کے لیے سرکاری خزانہ کے ساتھ ساتھ اپنے ذاتی سرمایہ سے امداد عطا فرمائے۔ لاوارث یتیم و بیسرا اطفال کو صنعت و حرفت کی مفت تعلیم و رہائش کا انتظام کیے، تاکہ مستقبل میں باعزتی کے ساتھ خوشحال زندگی گزار سکے۔ اسی طرح لاوارث یتیم و بیسرا لڑکیوں کی نگہداشت کے لیے خواتین اساتذہ کی نگرانی میں مفت رہائش، تعلیم و تربیت کے ساتھ ساتھ دستکاری کی تربیت دی۔

امیر پائیگاہ سرآسمان جاہ نے رعایا پروری کے ہر گوشہ میں نمایاں خدمات انجام دیے ہیں۔ سلطنت کا کوئی گوشہ ان کے خدمات سے خالی نہیں ہے۔ ان کے خدمات ملک کے شہریوں کے ساتھ احسان عظیم کے ساتھ بنی نوع انسان کی ہمدردی کا ثبوت دیا۔ ان کی خیرخواہی، دریادلی، داد و دہش میں ان کا کوئی ثانی نہیں۔